A Passive Optical Transmitter Using LC Switches for IoT Smart Dusts

Jingjing Liu
Shenzhen SoC Key Laboratory
PKU-HKUST Shenzhen-HK Institution
Shenzhen, China
liujingjing0428@163.com

Riqing Chen
Digital Fujian Institute of Agriculture and Forestry
Fujian Agriculture and Forestry University
Fuzhou, China
riqing.chen@fafu.edu.cn

Yuan Ren
Shenzhen SoC Key Laboratory
PKU-HKUST Shenzhen-HK Institution
Shenzhen, China
elwinry@hotmail.com

Zhongting Xu
Shenzhen SoC Key Laboratory
PKU-HKUST Shenzhen-HK Institution
Shenzhen, China
414684317@qq.com

Guoqing Hu
Shenzhen SoC Key Laboratory
PKU-HKUST Shenzhen-HK Institution
Shenzhen, China
hukingkkk@163.com

Jun Pan
Shenzhen SoC Key Laboratory
PKU-HKUST Shenzhen-HK Institution
Shenzhen, China
523360114@qq.com

Chunlai Li
Shenzhen SoC Key Laboratory
PKU-HKUST Shenzhen-HK Institution
Shenzhen, China
lpchunlai@yahoo.com

Jin He
Shenzhen SoC Key Laboratory
PKU-HKUST Shenzhen-HK Institution
Shenzhen, China
frankhe@pku.edu.cn

***Abstract*—Using optical wireless communications for sensors enables low power and small size of the nodes, such as smart dusts. This paper proposes a passive optical transmitter for smart dusts. Two liquid crystal (LC) modulator circuits have been designed for the switching the liquid crystal cells in the transmitter. The circuits are fabricated using a standard 0.18µm CMOS process. Measurement results show that they can work under 0.5V supply and successfully do the switching as designed. The transmission data rate can be 10bps, which is limited by the response speed of the LC cell.**

Keywords*—*Internet of Things, optical transmitter, smart dusts, liquid crystal cell

I. Introduction

The Internet of Things (IoT) draws more and more attentions due to its broad applications. The IoT will consist of billions of sensors to ensure the coverage and connectivity. When a sensor node integrates self-contained sensing and communication system into a cubic-millimetre mote, it is called "Smart Dust" [1-3]. Oxford developed an optical wireless communication network system including a base station and smart dust motes (SDMs) [4-8]. The structure of the SDM is shown in Fig. 1. It consists of on-chip solar cells, a storage capacitor, an optical receiver, an LC modulator and a modulated retro-reflector (MRR). The solar cells scavenge energy from the laser illumination and environment and the storage capacitor is connected in parallel to the solar cells. The optical receiver can detect the optical signals modulated onto the downlink beam, recover the clock and data, decode instructions and generate an output. Since sensors are not considered in this version of SDM, the receiver output directly drives the LC modulator of the optical transmitter. When the laser illuminates the SDMs, the MRR retro-reflects the beam back to the BS. Therefore the MRR allows the transmission of information from SDM to the BS. This paper focuses on the design of passive optical transmitter on the SDM.

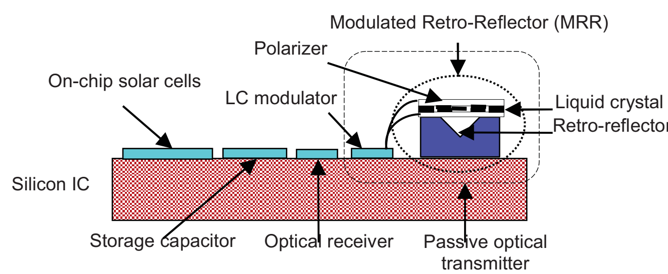

Fig. 1. The structure of SDM.

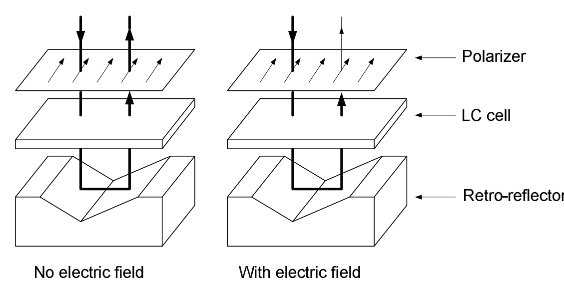

Fig. 2. The passive transmitter on the smart dust works with electric fields and without electric fields across the LC cell.

II. Design of Passive optical Transmitter

The MRR on the SDM is composed of a polarizer, a LC cell and a retro-reflector as shown in Fig. 2. The laser goes through the polarizer and a polarized light enters the LC cell. The light goes through the LC cell first, then is reflected back by the retro-reflector, and finally comes out of the LC cell. If there is no electric field, the light coming out of the LC cell passes through the polarizer and can be received by the base

978-1-7281-0319-8/19/$31.00 ©2019 IEEE

station. If there is an electric field across the LC, the polarization of the light coming out of the LC cell is rotated and thus a portion of light is blocked by the polarizer.

A. Liquid Crystal Cells

Some different LC cells have been developed, including hybrid aligned nematic (HAN) and anti-parallel alignment cells. Due to time limitations, only the ILC with anti-parallel alignment was optically tested as this liquid crystal has 0V threshold voltage and a large optical response, and is therefore likely to be the best choice for this application. Fig. 3 shows the measurement result of this liquid crystal. Fig. 3 (a) is a dc-balanced driving voltage with 0.5V amplitude and 10Hz frequency obtained from a function generator. Fig. 3 (b) is the detected signal by a photodetector and it shows the liquid crystal has a similar response for the two opposite electric field with the same strength.

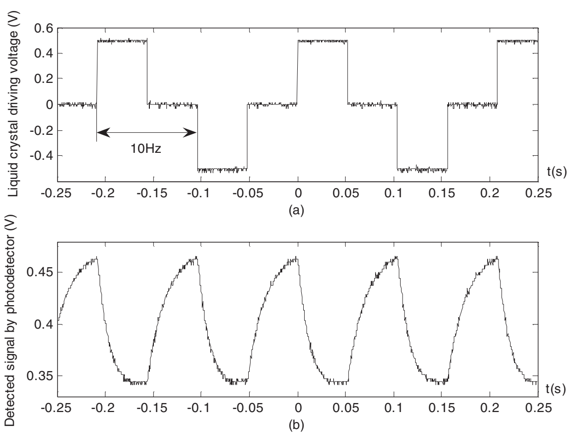

Fig. 3 Measurement results of ILCs with anti-parallel alignment, which has 0V Vth. (a) Liquid crystal driving voltage, (b) detected signal by a photodetector.

B. LC Modulator1

LC modulators are used to switch the liquid crystals. The input to the modulator is the output of the optical receiver, and there are two outputs, which will be connected to the LC cell. The output voltage difference of LC modulator1 switches between V_{dd} and - V_{dd} and it can be used for the ILCs with a non-zero threshold voltage. The threshold voltage will make the liquid crystal switch asymmetrically under the two opposite fields.

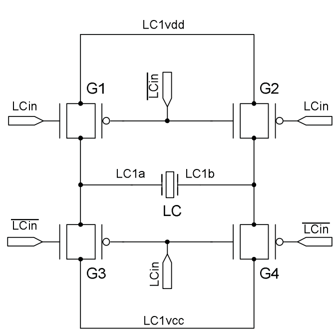

Fig. 4. Circuit diagram of LC modulator1.

Fig. 4 shows the circuit diagram of LC modulator1, which consists of 4 transmission gates, G1-G4. If LCin is high, G1 and G4 conduct, G2 and G3 are open loop. LC1a and LC1b are connected to LC1vdd and LC1vcc respectively. The direction of the electric field across the LC is from left to right. If LCin is low, G1 and G4 are open loop, G2 and G3 conduct. LC1a and LC1b are connected to LC1vcc and LC1vdd respectively. The field across the LC is now opposite and has the same strength as before. Fig. 5 shows the simulation results for LC modulator1 with 0.5V supply and 10Hz input. The voltage across the LC changes by twice that of the voltage rail. The total simulated current consumption is approximately 2.005nA. In each time period, the LC switches twice and both switches consume current from the power supply. The switching of the 100pF capacitor consumes 2nA average current.

$$I = {}^{nCU}\!/_{1s} = 10\,Hz \times 2 \times 100\ pF \times 1V = 2nA \qquad (1)$$

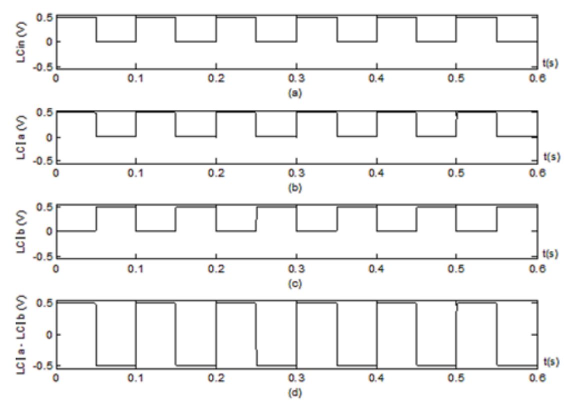

Fig. 5 Simulation results of LC modulator1. (a) LCin, (b) LC1a, (c) LC1b, (d) LC1a-LC1b.

C. LC Modulator2

The LC modulator2 can switch a liquid crystal with 0V threshold voltage into four stages, no electric field, positive field, no electric field and negative field. This modulator can be used to drive the ILCs with 0V threshold voltage. LC modulator2 uses four gates to switch the LC cell shown in Fig. 6. The LC cell is switched in such a sequence that the voltage across the LC is 0, V_{dd}, 0 and $-V_{dd}$. For example, in the initial state LC2a and LC2b are both connected to LC2vcc and the voltage in the LC is 0V. In the second state, LC2a is still connected to LC2vcc but LC2b is connected to LC2vdd. Thus the voltage across the LC is V_{dd}. In the third state, LC2a and

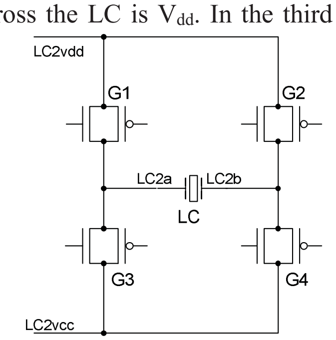

Fig. 6. Four gates control the LC cell in the LC modulator2.

LC2b are both connected to LC2vdd and there is 0V across the LC cell again. In the final state, LC2a and LC2b are connected to LC2vdd and LC2vcc respectively. The voltage direction is opposite to the second state and thus it can be regarded as $-V_{dd}$. The next state switches back to the first state, and causes the four states to repeat.

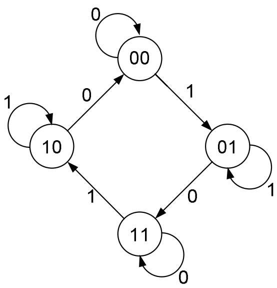

Fig. 7. State diagram of LC modulator2.

Therefore there are two state variables, LC2a and LC2b, which represent the two terminal voltages of LC cell. If the state variable is “1”, it means the terminal is connected to the LC2vdd. If the state variable is “0”, it means the terminal is connected to the LC2vcc. The state diagram of LC modulator2 is obtained, as shown in Fig. 7. The digit on the arrow represents the modulator input LCin. If the input is “0”, it means there is no voltage across the LC cell. If the input is “1”, it means voltage is applied across the cell. To avoid a short circuit between LC2vdd and LC2vcc, G1 and G3 should not conduct at the same time. Similarly, G2 and G4 should not conduct at the same time. This means

$$G3 = \overline{G1}\,,\ G4 = \overline{G2} \tag{2}$$

It is only necessary to design the logic circuits for G1 and G2. LC modulator2 needs two D flip flops to represent the two state variables. The logic circuits connected to the inputs of the two flip flops are represented in (4) and (5). Except NOT gates, all the logics are implemented by NAND gates for design convenience.

$$D1 = \overline{\left(\overline{LC2b_t \cdot \overline{LC2a_t} \cdot \overline{\overline{LCin}}}\right) \cdot \left[\overline{LC2a_t\left(\overline{\overline{LC2b_t} \cdot \overline{\overline{LCin}}}\right)}\right]} \tag{4}$$

$$D2 = \overline{\left(\overline{LC2b_t \cdot LC2a_t \cdot \overline{\overline{LCin}}}\right) \cdot \left[\overline{\overline{LC2a_t}\left(\overline{\overline{LC2b_t} \cdot \overline{\overline{LCin}}}\right)}\right]} \tag{5}$$

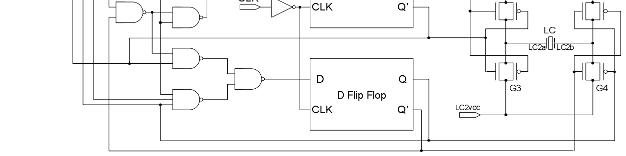

Fig. 8. Circuit diagram of LC modulator2.

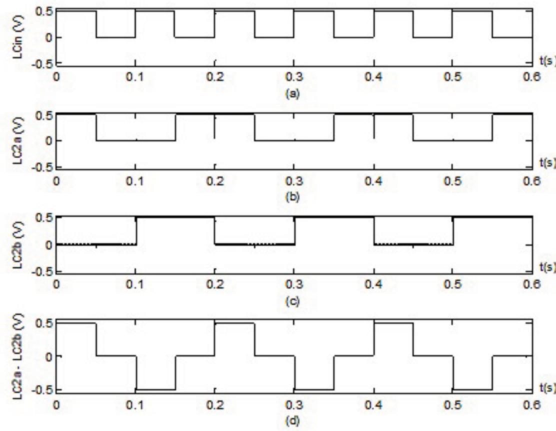

Fig. 9 Simulation results of LC modulator2. (a) LCin, (b) LC2a, (c) LC2b, (d) LC2a-LC2b.

The circuit diagram of LC modulator2 is shown in Fig. 8. The circuit needs a clock signal for the flip flops and it can be obtained from the optical receiver. The simulation results for 10Hz frequency input and 0.5V supply are shown in Fig. 9. The voltage across the LC cell in Fig. 9 (d) is dc balanced, which matches the design requirement. The voltage at LC2a has glitches at 0.2s and 0.4s. Just before the glitches, the voltage across the LC is 0V. At the instant of 0.2s or 0.4s, LC2b is switched from LC2vdd to LC2vcc. In order to keep the zero field in the LC cell, the node voltage at the LC2a will follow the voltage at the LC2b and decrease. Then the LC2a node voltage is charged up through G1 from LC2vdd. Simulation results show that the total current consumption of the LC modulator2 is approximately 955pA. The switching of the 100pF capacitor consumes 500pA average current as shown in (6). This means the logic circuits consume approximately 455pA for a 0.5V supply.

$$I = {CU}/{1s} = 10\ Hz \times 100\ pF \times 0.5V = 500\ pA \tag{6}$$

III. Measurement Results

The two LC modulators were fabricated using a standard 0.18μm CMOS process. The outputs of LC modulators are designed to be connected to the LC cell. Therefore they are not buffered and cannot be directly connected to oscilloscopes for measurements. This is because the high impedance port of the oscilloscope has an impedance of 1MΩ respect to the ground and the port will sink micro-Amperes from the circuits, which is a significant current for the low power design. As a result, two off-chip opamp buffers on a PCB are used as the LC modulator output buffers in the measurement. The measurement results for LC modulator1 with a 0.5V supply is shown in Fig. 10. They match with the simulation results, therefore LC modulator1 works as expected. Fig. 11 shows the measurement results for LC modulator2 with a 0.5V supply. The measurement results are similar to the simulation results except that there are no glitches in the second signal. This is because the modulator outputs only drive the off-chip buffers and there is no 100pF capacitor connected to the outputs.

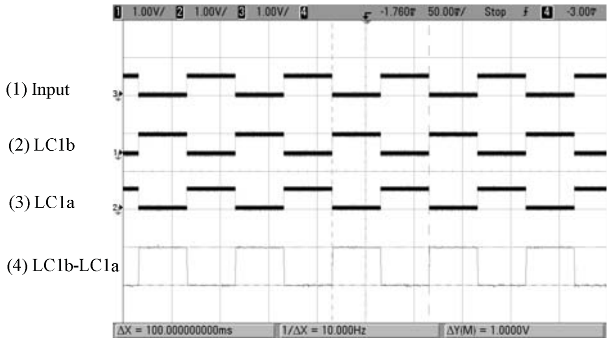

Fig. 10 Measurement results of LC modulator1.

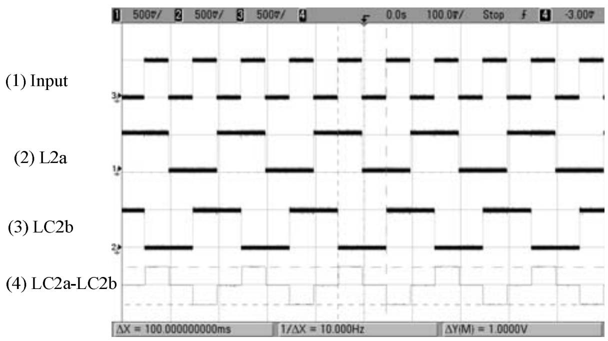

Fig. 11 Measurement results of LC modulator2.

IV. CONCLUSIONS

This paper discusses a passive optical transmitter for IoT smart dust applications. The optical transmitter consists of a MRR and LC modulator circuits. Two different modulator circuits are designed to switch the ionic liquid crystal cell in the MRR. The LC modulator1 can be used to switch the LC cells with non-zero threshold voltage, while the LC modulator2 can be used to switch the LC cell with 0V threshold voltage. The circuits were fabricated using a standard 0.18μm CMOS process. Measurement results show that they can work under 0.5V supply and do the switching as designed.

ACKNOWLEDGMENT

This work was supported by UK Engineering and Physical Sciences Research Council (EPSRC) under Grant No. EP/D501008/1 and Shenzhen funding under Grant No. JCYJ20170817112848591, JCYJ20180227175343343 and JCYJ20170817113029596.

REFERENCES

[1] B. Warneke, B. Liebowitz, and K. S. J. Pister, “Smart dust: Communicating with a cubic-millimeter computer,” Computer, vol.34, issue1, pp. 44-51, January 2001.

[2] B. Warneke, B. Atwood, and K. S. J. Pister, “Smart dust mote for runners,” Proceedings of the 14th IEEE International Conference on MEMS, Interlaken, Switzerland, January 2001.

[3] J. M. Kahn and K. S. J. Pister, “Next century challenges: Mobile networking for ‘Smart Dust’,” Proceedings of the 5th Annual ACM/IEEE International Conference on Mobile Computing and Networking, Seattle, United States, pp. 271-278, 1999.

[4] J. J. Liu, G. E. Faulkner, B. Choubey, J. Liu, R. Q. Chen, D. C. O'Brien and S. Collins, "Optically Powered Energy Source in a Standard CMOS Process for Integration in Smart Dust Applications," IEEE Journal of Electron Devices Society, .vol. 2, No. 6, pp. 158-163, Nov. 2014.

[5] J. J. Liu, Y. M. Zhou, G. F. Faulkner, D. C. O'Brien and S. Collins, "Optical receiver front end for optically powered smart dust", International Journal of Circuit Theory and Applications, vol. 43, issue 7, pp. 840-853, July 2015.

[6] J. J. Liu, G. E. Faulkner, B. Choubey, S. Collins and D. C. O'Brien, "A tunable passband logarithmic photodetector for IoT smart dusts", IEEE Sensors Journal, vol. 18, issue 13, pp. 5321-5328, July, 2018.

[7] J. J. Liu, G. E. Faulkner, B. Choubey, S. Collins and D. C. O'Brien, "An optical transceiver powered by on-chip solar cells for IoT smart dusts with Optical Wireless Communications ", early access in IEEE Internet of Things Journal, doi: 10.1109/JIOT.2018.2881424.

[8] D. C. O’Brien, J. J. Liu, G. E. Faulkner, S. Sivathasan, W. W. Yuan, S. Collins, S. J. Elston and V. Pithamiron, “Design and implementation of optical wireless communications with optically powered smart dust motes”, IEEE Journal on Selected Areas in Communications, vol. 27, No. 9, pp. 1646-1653, Dec. 2009.